



INTERNATIONAL APPLICATION PUBLISHED UNDER THE PATENT COOPERATION TREATY (PCT)

(51) International Patent Classification ⁷ : G06F 19/00		A2	(11) International Publication Number: WO 00/52625
			(43) International Publication Date: 8 September 2000 (08.09.00)
(21) International Application Number: PCT/US00/04076		(81) Designated States: AE, AL, AM, AT, AU, AZ, BA, BB, BG, BR, BY, CA, CH, CN, CR, CU, CZ, DE, DK, DM, EE, ES, FI, GB, GD, GE, GH, GM, HR, HU, ID, IL, IN, IS, JP, KE, KG, KP, KR, KZ, LC, LK, LR, LS, LT, LU, LV, MA, MD, MG, MK, MN, MW, MX, NO, NZ, PL, PT, RO, RU, SD, SE, SG, SI, SK, SL, TJ, TM, TR, TT, TZ, UA, UG, US, UZ, VN, YU, ZA, ZW, ARIPO patent (GH, GM, KE, LS, MW, SD, SL, SZ, TZ, UG, ZW), Eurasian patent (AM, AZ, BY, KG, KZ, MD, RU, TJ, TM), European patent (AT, BE, CH, CY, DE, DK, ES, FI, FR, GB, GR, IE, IT, LU, MC, NL, PT, SE), OAPI patent (BF, BJ, CF, CG, CI, CM, GA, GN, GW, ML, MR, NE, SN, TD, TG).	
(22) International Filing Date: 17 February 2000 (17.02.00)			
(30) Priority Data: 09/253,789 22 February 1999 (22.02.99) US			
(71) Applicant (for all designated States except US): VIALOGY CORPORATION [US/US]; 2400 Lincoln Avenue, Altadena, CA 91001 (US).			
(72) Inventor; and			
(75) Inventor/Applicant (for US only): GULATI, Sandeep [IN/US]; 5467 La Forest Drive, La Canada, CA 91011 (US).			
(74) Agents: KUKKONEN, Carl, A., III et al.; Pretty, Schroeder & Poplawski, 19th floor, 444 South Flower Street, Los Angeles, CA 90071 (US).			

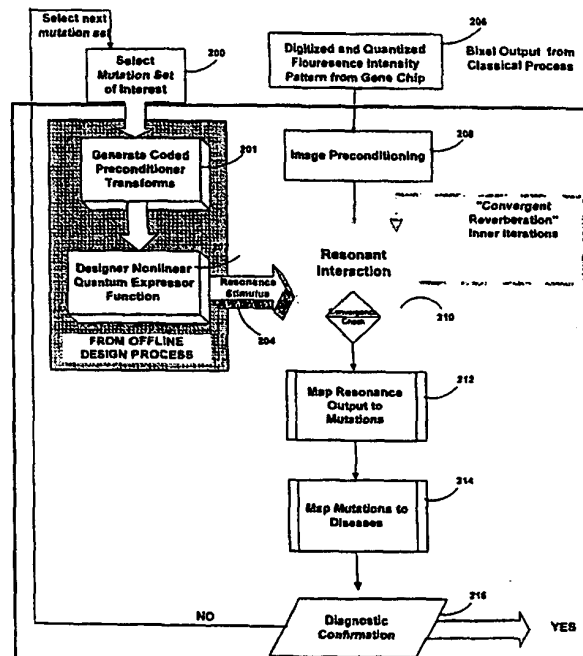
Published

Without international search report and to be republished upon receipt of that report.

(54) Title: METHOD AND APPARATUS FOR ANALYZING HYBRIDIZED BIOCHIP PATTERNS USING RESONANCE INTERACTIONS

(57) Abstract

A technique is described for identifying mutations, if any, present in a biological sample, from a pre-selected set of known mutations. The method can be applied to DNA, RNA and peptide nucleic acid (PNA) microarrays. The method analyzes a dot spectrogram representative of quantized hybridization activity of oligonucleotides in the sample to identify the mutations. In accordance with the method, a resonance pattern is generated which is representative of nonlinear resonances between a stimulus pattern associated with the set of known mutations and the dot spectrogram. The resonance pattern is interpreted to a yield a set of confirmed mutations by comparing resonances found therein with predetermined resonances expected for the selected set of mutations. In a particular example, the resonance pattern is generated by iteratively processing the dot spectrogram by performing a convergent reverberation to yield a resonance pattern representative of resonances between a predetermined set of selected Quantum Expressor Functions and the dot spectrogram until a predetermined degree of convergence is achieved between the resonances found in the resonance pattern and resonances expected for the set of mutations. The resonance pattern is analyzed to a yield a set of confirmed mutations by mapping the confirmed mutations to known diseases associated with the pre-selected set of known mutations to identify diseases, if any, indicated by the biological sample. By exploiting a resonant interaction, mutation signatures may be robustly identified even in circumstances involving low signal to noise ratios or, in some cases, negative signal to noise ratios.



**METHOD AND APPARATUS FOR ANALYZING HYBRIDIZED BIOCHIP
PATTERNS USING RESONANCE INTERACTIONS EMPLOYING QUANTUM
EXPRESSOR FUNCTIONS**

5

Field of the Invention

The invention generally relates to techniques for analyzing biological samples such as DNA, RNA, or protein samples and in particular to techniques for analyzing the output patterns of hybridized biochip microarrays.

Background of the Invention

10

A variety of techniques have been developed to analyze DNA or other biological samples to identify diseases, mutations, or other conditions present within a patient providing the sample. Such techniques may determine, for example, whether the patient has any particular disease such as cancer or AIDS, or has a predisposition toward the disease, or other medical conditions present in the patient. DNA-based analysis may be used either as an in-vitro or as an in-vivo control mechanism to monitor progression of disease, assess effectiveness of therapy or be used to design dosage formulations. DNA-based analysis is used verify the presence or absence of expressed genes and polymorphisms.

15

One particularly promising technique for analyzing biological samples uses a DNA-based microarray (or microelectronics biochip) which generates a hybridization pattern representative of the characteristics of the DNA within the sample. Briefly, a DNA microarray includes a rectangular array of immobilized single stranded DNA fragments. Each element within the array includes few tens to millions of copies of identical single stranded strips of DNA containing specific sequences of nucleotide bases. Identical or different fragments of DNA may be provided at each different element of the array. In other words, location (1,1) contains a different single stranded fragment of DNA than location (1,2) which also differs from location (1,3) etc. Certain biochip designs may replicate the nucleotide sequence in multiple cells.

20

25

DNA-based microarrays deploy chemiluminescence, fluorescence or electrical phenomenology to achieve the analysis. In methods that exploit fluorescence imaging, a target DNA sample to be analyzed is first separated into individual single stranded sequences and fragmented. Each sequence being tagged with a fluorescent marker molecule. The fragments are applied to the microarray where each fragment binds only with complementary DNA fragments already embedded on the microarray. Fragments which do not match any of the elements of the microarray simply do not bind at any of the sites of the microarray and are discarded during subsequent fluidic reactions. Thus, only those microarray locations containing fragments that bind

30

for analyzing the output thereof will now be described in greater detail. Initially, at step 100, fluorescently labeled primers are prepared for flanking loci of genes of interest within the DNA sample. The primers are applied to the DNA sample such that the fluorescently labeled primers flank genes of interest. At step 102, the DNA sample is fragmented at the locations where the
5 fluorescently labeled primers are attached to the genes of interest to thereby produce a set of DNA fragments, also called "oligonucleotides" for applying to the DNA microarray.

In general, there are two types of DNA microarrays: passive hybridization microarrays and active hybridization microarrays. Under passive hybridization, oligonucleotides characterizing the DNA sample are simply applied to the DNA microarray where they passively attach to
10 complementary DNA fragments embedded on the array. With active hybridization, the DNA array is configured to externally enhance the interaction between the fragments of the DNA samples and the fragments embedded on the microarray using, for example, electronic techniques. Within FIG. 1, both passive hybridization and active hybridization steps are illustrated in parallel. It should be understood that, currently for any particular microarray, either the passive hybridization or the
15 active hybridization steps, but not both, are typically employed. Referring first to passive hybridization, at step 104 a DNA microarray chip is prefabricated with oligonucleotides of interest embedded or otherwise attached to particular elements within the microarray. At step 106, the oligonucleotides of the DNA sample generated at step 102 are applied to the microarray. Oligonucleotides within the sample that match any of the oligonucleotides embedded on the
20 microarray passively bind with the oligonucleotides of the array while retaining their fluorescently labeled primers such that only those locations in the microarray having corresponding oligonucleotides within the sample receive the primers. It should be noted that each individual nucleotide base within the oligonucleotide sequence (with lengths ranging from 5 to 25 base pairs) can bond with up to four different nucleotides within the microarray, but only one oligonucleotide
25 represents an exact match. When illuminated with fluorescent light, the exact matches fluoresces most effectively and the non-exact matches fluoresce considerably less or not at all.

At step 108, the DNA microarray with the sample loaded thereon is placed within a fluidics station provided with chemicals to facilitate the hybridization reaction, i.e., the chemicals facilitate the bonding of the oligonucleotide sample with corresponding oligonucleotides within the
30 microarray. At step 110, the microarray is illuminated under fluorescent light, perhaps generated using an ion-argon laser, and the resulting fluorescent pattern is digitized and recorded. Alternately, a photograph of the fluorescent pattern may be taken, developed, then scanned into a computer to provide a digital representation of the fluorescent pattern. In any case, at step 112, the digitized pattern is processed using dedicated software programs which operate to focus the digital

Classical methods such as probabilistic estimator such as minimum a posteriori (MAP) estimator, maximum likelihood estimator (MLE) or inferencing mechanism may be used to render a diagnostic assessment.

As noted above, it would be desirable to provide improved techniques for analyzing the
5 outputs for DNA microarrays to more quickly, reliably and inexpensively yield a valid diagnostic assessment. To this end, the invention is directed primarily to providing a sequence of steps for replacing steps 114-130 of FIG. 1.

Summary of the Invention

10 In accordance with a first aspect of the invention, a method is provided for analyzing an output pattern of a biochip to identify mutations, if any, present in a biological sample applied to the biochip. In accordance with the method, a resonance pattern is generated which is representative of resonances between a stimulus pattern associated with a set of known mutations and the output pattern of the biochip. The resonance pattern is interpreted to yield a set of
15 confirmed mutations by comparing resonances found therein with predetermined resonances expected for the selected set of mutations.

In an exemplary embodiment, the biological sample is a DNA sample and the output pattern being analyzed is a quantized dot spectrogram generated by a hybridized oligonucleotide microarray. The resonance pattern is generated by iteratively processing the dot spectrogram by
20 performing a convergent reverberation to yield a resonance pattern representative of resonances between a predetermined set of selected Quantum Expressor Functions and the dot spectrogram until a predetermined degree of convergence is achieved between the resonances found in the resonance pattern and resonances expected for the set of mutations. The resonance pattern is analyzed to yield a set of confirmed mutations by mapping the confirmed mutations to known
25 diseases or diagnostic conditions of interest, associated with the pre-selected set of known mutations to identify diseases, if any, indicated by the DNA sample. A diagnostic confirmation is then made by taking the identified diseases and solving in reverse for the associated Quantum Expressor Functions and then comparing those Quantum Expressor Functions with ones expected for the mutations associated with the identified disease to verify correspondence. If no
30 correspondence is found, a new sub-set of known mutations are selected and the steps are repeated to determine whether any of the new set of mutations are present in the sample.

In the exemplary embodiment the set of nonlinear Quantum Expressor Functions are generated are follows. A set of mutation signatures representative of the pre-selected set of known mutations is input. A representation of a microarray oligonucleotide pattern layout for the

various arrayed biomolecular, ionic, bioelectronic, biochemical, optoelectronic, radio frequency (RF) and electronic microdevices. Principles of the invention are particularly applicable to mutation expression analysis at ultra-low concentrations using ultra-high density passive and/or active hybridization DNA-based microarrays. Techniques implemented in accordance with the invention are generally independent of the physical method employed to accumulate initial amplitude information from the bio-chip array, such as fluorescence labeling, charge clustering, phase shift integration and tracer imaging. Also, principles of the invention are applicable to optical, optoelectronic, and electronic readout of hybridization amplitude patterns. Furthermore, principles of the invention are applicable to molecular expression analysis at all levels of abstraction: namely DNA expression analysis, RNA expression analysis, protein interactions and protein – DNA interactions for medical diagnosis at the molecular level.

Apparatus embodiments are also provided.

Brief Description of the Drawings

The features, objects, and advantages of the present invention will become more apparent from the detailed description set forth below when taken in conjunction with the drawings in which like reference characters identify correspondingly throughout and wherein:

Fig. 1 is a flow chart illustrating conventional passive and active hybridization DNA microarray analysis techniques.

Fig. 2 is a flow chart illustrating an exemplary method for analyzing the output of a hybridized DNA microarray in accordance with the invention.

Fig. 3 graphically illustrates the method of Fig. 2.

Fig. 4 is a flow chart illustrating an exemplary method for generating Quantum Expressor Functions for use with the method of Fig. 2.

Fig. 5 is a flow chart illustrating an exemplary method for preconditioning the output of a hybridized DNA microarray for use with the method of Fig. 2.

Detailed Description of Exemplary Embodiments

With reference to the remaining figures, exemplary embodiments of the invention will now be described. The invention will be described primarily with respect to an exemplary method for analyzing mutations signatures within output patterns of hybridized microarrays generated using DNA samples, but principles of the invention apply to the analysis of other protein-based samples or to other types of output patterns as well.

Overview

exploitation of resonance suppressors to verify detection.

The Method

Referring first to **FIG. 2**, initially at step **200**, a set of mutations of interest is selected. The mutations, for example, may be mutations relevant to cancer, AIDS, or other diseases or medical conditions. At step **201**, preconditioner transforms are generated based upon the selected set of mutations. The preconditioner transforms are provided to convert mutation nucleotide sequences into expected amplitude patterns in the prespecified microarray representation, given a particular biochip layout. At step **202**, Quantum Expressor Functions are generated based upon the Hamiltonian of a pre-selected basis system. The Quantum Expressor Functions are designed to couple the Hamiltonian for the selected basis system to a predetermined DNA microarray configuration to permit a resonance interaction involving the output of the DNA microarray. Resonance stimulus is generated, at step **204**, using the Quantum Expressor functions.

What has been summarized thus far are preliminary steps performed off-line for setting up the Quantum Expressor Functions and the corresponding resonance stimulus. These steps need be performed only once for a given set of mutations and for a given DNA microarray configuration. Thereafter, any number of output patterns from the DNA microarray may be processed using the Quantum Expressor Functions to identify whether any of the mutations of the pre-selected set of mutations are found therein. Preferably, Quantum Expressor Functions are pre-generated for a large set of mutations and for a large set of DNA microarray patterns such that, for each new DNA microarray output pattern from each new patient sample, the presence of any of the mutations can be quickly identified using the predetermined set of Quantum Expressor Functions. In general, the aforementioned steps need be repeated only to update the Quantum Expressor Functions to accommodate new and different DNA microarray patterns or to if new mutations of interest need to be considered.

At step **206**, an output pattern (referred to herein as a Dot Spectrogram) is generated using a DNA microarray for which Quantum Expressor Functions have already been generated. At step **208**, the dot spectrogram is preconditioned to yield a dot spectrogram tessellation (DST) to permit exploitation of a resonance interaction between the dot spectrogram and the Quantum Expressor Functions. The actual resonant interaction, which involves convergent reverberations, is performed at step **210** until a pre-determined degree of convergence is achieved. Once convergence is achieved, a resulting resonance pattern is processed at step **212** to identify any mutations represented thereby. As will be described below, step **212** is rendered trivial by virtue of the aforementioned resonant interaction which is based upon Quantum Expressor Function already correlated with the pre-selected mutations. Hence, no complicated analysis is required to interpret

signal-to-noise ratio (SNR)=0.

In the exemplary embodiment, the DNA microarray is an N by M DNA chip array wherein an element of the array is referred to herein as an "oxel": $o(i,j)$.

The pre-hybridization microarray (PEBC) is expressed as:

$$5 \quad PEBC = \sum_1^N \sum_1^M o(i,j), \text{ where } N \text{ and } M \text{ refer to the linear (row and column)}$$

dimensions of the 2-D microarray.

An inverse Dirichlet Tessellation (IDT) on the PEBC is applied such that a singular value decomposition (SVD) on the resulting array yields the location of the mutation of interest at the SNR=0 condition. Conceptually the process corresponds to setting up a concave diffusion front at
10 the mutation-centered oxel.

The equations used are

$$x_f = k_x (Dt)^{1/2}$$

$$15 \quad \sigma_f = k_\sigma (Dt)^{\alpha_\sigma/2} \text{ where } \alpha_\sigma = 4/7.$$

$$N_f = k_N L (Dt)^{\alpha_N/2} \text{ where } \alpha_N = 3/7.$$

$$D_H = 7/4.$$

20 The constants k_x , k_σ and k_N are respectively set to 0.856, 0.68, and 1.34, and for biochip dimensions $N, M > 100$, t is typically set to $10^2 * a^2/D$ where a = inter-oxel distance and D is a coefficient for percolation of the point spread. D is chosen as 0.001. These equations impose a specific IDT, i.e., rapid diffusion on the mutation-centered oxel, and synthetically tessellate the biochip.

25

Basis System for Quantum Expressor Functions

To generate Quantum Expressor Functions (QEF) at step 202, a basis system for the QEF is first selected. The selection of the basis system and the generation of the QEF's based thereon depends, in part, and the characteristics of the DNA microarray.

30 The numeric value associated with each oxel is given by:

$$\hat{O}(i,j) = \alpha_k \cdot 4^{k-1} + \alpha_{k-1} \cdot 4^{k-2} + \dots + \alpha_1 \cdot 4^1 + \alpha_0 \cdot 4^0$$

quantum noise is exploited to drive order in a quantum-mechanical system, as opposed to Gaussian noise in a classical system. The appearance of a resonance requires an asymmetry in the energies of the two states. A rate equation can be constructed for the system, such that the dynamics can be characterized in terms of transition rates Φ_+ and Φ_- between the two asymmetric quantum superposition states, and when the drive frequency and the interwell transition rates are much slower than the intrawell relaxation rates. The signal to noise ratio (SNR) of such a superposition system is given by:

$$SNR = \frac{\pi}{4} \frac{\Phi_{+0}}{1 + \exp[\epsilon_0 / \kappa_B T_0]} \left[\delta \left[\frac{\epsilon}{\kappa_B T} \right] \right]^2 \epsilon$$

Where κ_B is the Boltzmann's constant, and T is the temperature. The sinusoidally

$$\epsilon = \epsilon_0 + \delta_\epsilon \times \cos \omega_s t$$

modulated asymmetry energy ϵ is given by:

$$C(\tau) = \langle n_+(t+\tau | q_+, t) n_+(t | q_0, -\infty) \rangle$$

In the above expression the power spectrum $S(\omega)$ represents the Fourier transform of $C(\tau)$, containing a roughly Lorentzian broadband noise background and δ -function peaks at $\omega = 0$, the driving frequency ω_s , and its harmonics. The measured correlation function for the quantum noise is given by $C(t) = \langle n_{+i}(t) n_{+i}(t + \tau) \rangle$, where each $n_{+i} = 0$ or 1, and the \langle , indicates an average over t over many data points i taken at equal intervals.

The probability of being in the + quantum state at t after being in the state q_0 at is given by

$$n_+(t | q_0, -\infty).$$

QSR occurs for an asymmetric well, but not for a symmetric energy well.

A custom Hamiltonian, for use with step 402, which couples the above system to an ensemble of harmonic oscillators is given by

equilibrium state in the absence of driving force.

The power amplitudes η_m in the m th frequency component of asymptotic state space are calculated at step 404 using

$$\eta_m(\Omega, \varepsilon) = 4\pi |P_m(\Omega, \varepsilon)|$$

and the phase shift is given by

$$\varphi_m(\Omega, \varepsilon) = \tan^{-1} \left[\frac{\text{Im}(P_m(\Omega, \varepsilon))}{\text{Re } P_m(\Omega, \varepsilon)} \right]$$

10

The analytic for the external force is given by

$$P_m(\Omega, \varepsilon) = \frac{\gamma}{\gamma - i m \Omega} \frac{2\omega_c}{\pi} h(-i m \Omega, \gamma)$$

15

The parameters γ , ε_0 are predetermined and are design specific. Typically, values of 0.001 and 0.0001 are used for γ and ε_0 respectively. In the above expression $|P_m|$ determine the weights of the δ spikes of the averaged spectral power density.

For particular applications, the QEF is designed by matching the power spectral density (PSD) amplitude of coded mutation signature to that of the spin-boson system described above so that stochastic and deterministic time scales match and so that the time scales couple back to noise statistics and degree of asymmetry. The method employs a fully automated iterative conjugate gradient relaxation method for Spectral matching between asymmetric base system and coded mutation signature. The actual determination of the QEF depends on the specifics of bioelectronics substrates used for actual analysis. The method is however generalizable to all or almost all arrayed embodiments. In addition, the method is highly scalable to array dimensions (as the offline design trade-space time does not matter to computational complexity). Since the system is an overdetermined coupled system, convergence criteria and stability of relaxation method directly relates to downstream resonance effectiveness.

30

nonlinear oscillators, wherein a number of different entrained states co-exist. At ground truth POBC locations, an *a priori* measurement of entrainment is performed (step 408). This is done by approximate Daido Integral() with Z_k = PSD maxima at regions where DST boundary > desired detection threshold. (For more information regarding the Daido Integral, see Physics Review Letters, 77(7), 1406-1411.) Premultiplier constants are used to ensure that Z_k meets the following tests:

- maxima power spectrum density (PSD) matches; and
- L_2 norm on even harmonics < e where e = NS-MRF Barrier assuming CSR assumptions.

10

The notion of entrainment states is exploited, in part, because the method treats the hixel dot spectrogram as a special case of coupled nonlinear oscillators in equilibrium. However, due to device imperfections, hybridization degradation and other limitations number of entrained binding states (i.e., incorrectly hybridized) coexist. A PSD match is desired where the OF is Z-peaked (but single peaked around each MRC-hixel). Absence of a single peak implies perfect or lack of hybridization. It also defines the resonance loci for this method (i.e., where maximum SNR enhancement) is obtained.

15

Ground Truth Modulation

20

The OF of ground truth is modulated at step 410 to yield the QEF as follows. Under controlled calibration, as stated above, maximal SNR enhancement (optimal resonance) is achieved when OF yields a single peak. It is a important design point for matching PSD of coupling spin Boson system to the synthetic QEF. The specific form of the QEF to be used is the generic OF shown above. So the exemplary method exploits two connotations of OF: (a) parametric form for the QEF (that is closer to the classical form) and (b) as exponential attractor for a dissipative system. The two OF's are then recoupled and convolved with the preconditioned dot spectrogram (see below).

25

The resulting QEF generated via the steps of FIG. 4 is given by:

30

$$QEF_{MRC_i} = \tilde{H}(\tilde{\theta}) = - \sum_{j=I_x}^{u_x} \sum_{k=I_y}^{u_y} \hat{h}_{k|v_{i=1,2,3}} Z_k e^{-2mik\theta}$$

Typically, only first three PSD peaks are considered for spectral matching.

phase discontinuity and can be treated like a real-valued function. If values are computed for this deviation function $\text{err}(\cdot)$, then $|\text{err}(p)|$ would specify an intensity image whose local maxima might indicate detection of expressed oligonucleotides of interest.

Each phase angle corresponds to a point on the unit circle in the coordinate plane. This is a one-to-one mapping in both direction. Let V be the mapping that takes a phase angle into the corresponding vector on the unit circle. Let I be the inverse mapping that takes a vector on the unit circle back into the corresponding phase angle. $V(f(p))$ is thus a vector valued function which has no associated phase discontinuity. V can be averaged over a region without the problems associated with directly averaging phase angles.

Given a rectangular neighborhood $N(p,m,n)$ of the hixel p , let v be the vector which is the average of all the values of $V(f(p))$ in this region and let $|v|$ be the magnitude of this vector. Clearly $|v|$ must lie between 0 and 1, inclusive. Moreover, $|v|$ is a measure of the dispersion of the phase angles. If $|v|=1$, then all the vectors in the region $N(p,m,n)$ are equal to v . If $|v|=0$, then the vectors are distributed more or less uniformly about the unit circle and there is no "average" phase angle. If $|v|>0$, then $v/|v|$ is a vector on the unit circle and $I(v/|v|)$ can be defined to be the "average" phase angle $\text{ave}(f,p,m,n)$. Clearly, the closer $|v|$ is to 1, the tighter the clustering of the vectors about $v/|v|$ and the greater the certainty that this is a meaningful average value. The important characteristic is that this average will tolerate phase with data noise.

If the line is taken which is perpendicular to the vector v and passes through the point v , then this line will specify a chord of the unit circle. The arc of the unit circle which corresponds to this chord is the region from which the "average" vector comes. The length of this arc is $2 \cdot \arccos(|v|)$. Thus, to ensure that the "average" vector lies in a single quadrant or a 90 degree arc:

$$|v| = \cos(45 \text{ degrees}) = 0.7071$$

25

$|v|$ is referred to herein as the average magnitude and the minimum acceptable value for this average magnitude is referred to as minimum average magnitude.

Averaging Phase Input: Let f be a phase image, F the corresponding accumulated phase function, and $L+e=F$ be as described above. Assume that m and n are odd integers so that $N(p,m,n)$ is a symmetric $m \times n$ rectangle of hixels with p in the exact center. Since L is linear and $N(p,m,n)$ is symmetric about p , the average of L over $N(p,m,n)$ will be $L(p)$. Since $e = F-L$, the average of e over $N(p,m,n)$ should be close to 0. Hence, approximately,

These both define new phase images derived from f and are discrete analogs to the first derivative. The range of values for dv and df are also from -180 to $+180$.

Let F be the accumulated phase function corresponding to f and let $L+e=F$ be as described above. For the sake of convenience, assume that p is translated to the origin so that $p=(0,0)$. The
 5 linear function L is expressed as

$$L(i,j) = V*i + H*j + K$$

for some constants V , H , and K . If L is a reasonable approximation to F , then it is expected
 10 that the first vertical difference of f to be an approximation to the slope V and the first horizontal difference of f to be an approximation to the slope H . Hence it is possible to estimate V and H by averaging dv and dh over some appropriate rectangle centered at p . Let

$$\begin{aligned} V' &= \text{ave}(dv(f,p), p,m,n) \\ H' &= \text{ave}(dh(f,p), p,m,n) \end{aligned}$$

15

be these estimates. Note that these are phase averages. Probably m and n should be chosen so that m/n is roughly equal to H'/V' . This ratio would imply that the total phase accumulation across the rectangle $N(p,m,n)$ is about the same in both the vertical and horizontal directions. For
 20 example, the rate of change of phase along the i -axis (vertical) may be twice the rate of change along the j -axis (horizontal). In this case, a 5×10 rectangle of hixels may turn out to be the most appropriate neighborhood.

If a good estimate K' is computed for K , then an approximation to L is:
 25

$$L'(i,j) = V'*i + H'*j + K'$$

If L' is a good enough approximation to L and F is linear enough, then the accumulated phase function F is reconstructed as follows:

$$30 \quad e'(p) = f(p) - L'(p) \pmod{}$$

and

$$F(p) = L'(p) + e'(p)$$

a0 a1 a2 a3 a4 a5 a6

b0 b1 b2 b3 b4 b5

c1 c2 c3 c4 c5

5

where $b_0 = a_1 - a_0$, $b_1 = a_2 - a_1$, ... and $c_1 = b_1 - b_0$, $c_2 = b_2 - b_1$, ...

Let $F = L + e$ be defined as earlier. If e were identically 0, then F would be linear and both second differences $d2v$ and $d2h$ would also be identically 0. If e is not identically 0, the second differences will necessarily also deviate from 0, however, not necessarily in the same place as e . If $|e|$ attains a local maximum at a hixel p and this is associated with a very localized deviation from 0, as would be expected of a signal from a mutation of interest, then $d2v$ and $d2h$ should also deviate from 0 fairly nearby to p .

The deviation in $d2v$ and $d2h$ associated with a deviation in $|e|$ may be spread out over a number of hixels. This will not only make it harder to detect a significant change in $d2v$ and $d2h$ but also make it harder to locate the center of this change using a local maxima finding filter. It may be possible to compensate for this by averaging $d2v$ and $d2h$ or $|d2v|$ and $|d2h|$ over rectangular regions $N(p, m, n)$. This should tend to sharpen the peaks in $d2v$ and $d2h$. Correlating several different images generated using $d2v$ and $d2h$ may also help with center finding since the correlation algorithm will automatically average nearby local maxima.

Thus a method for achieving induced coupling for phase space has been described. Repeatability of the overall method hinges significantly on the aforementioned coupling as it induces analytic redundancy via complex information fusion at constant feed forward computational cost. Hence, the coupling is advantageous for at least two reasons: 1) it applies to any microarray device that may provide a phase or cyclical (modulo) input as opposed to amplitude input; and 2) it is important for use with active hybridization devices which will have an element of built in control that will have a phase representation. The coupling is actually introduced into the exemplary method in three possible ways.

(a) if the entire resonance computation proceeds in the phase space as opposed to amplitude space. Then it is necessary to transform QEF and post-hybridization microarray output to phase space. The coupling material provides the transformations to do so.

(b) if the microarray output is already in the phase space then it will only be applied to convert the QEF.

(c) if different oxels are designed to solve for different aspects of the analysis, the coupling

The post-hybridization microarray is treated mathematically using the machinery of equations with aftereffect. Each hixel given by $\Phi(i,j)$ is represented as a cluster of dynamical systems of potentially [CB] correctly bound, [UB] unbound, [PB] partially bound and [IB] incorrectly bound. Thus $[CB] \Phi(i,j) + [UB] \Phi(i,j) + [PB] \Phi(i,j) + [IB] \Phi(i,j) = T \Phi(i,j)$ within 0.0001%.

5 The model analytic for the estimated fluorescence activity $\hat{\Psi}$ in a hixel $h(i,j)$ is given by

$$\dot{\hat{\Psi}}_{h(i,j)}(t) = \Theta_{h(i,j)} \left(t, \Psi_{t,h(i,j)}, \dot{\Psi}_{t,h(i,j)} \right), \quad t \geq t_0 \text{ (hybridization start time).}$$

The fluorescence stabilization section is given by

10

$$\Psi_{t,h(i,j)} = \Psi_{h(i,j)}(t + \delta), \quad \delta \leq 0;$$

And the rate of fluorescence stabilization is expressed via

15
$$\dot{\Psi}_{t,h(i,j)} = \dot{\Psi}_{h(i,j)}(t + \delta), \quad \delta \leq 0;$$

While $\Theta \Psi_{t,h(i,j)} = \Psi_{h(i,j)}(t + \delta)$, $\delta \leq 0$; the system is assumed to be memoryless, i.e., Θ is ergodic.

20 The resulting dot spectrogram generated at step 206 is given by:

$$\Phi(i,j)$$

25

Preconditioning of The Dot Spectrogram

With reference to FIG. 5, the dot spectrogram $\Phi(i,j)$ is preconditioned by performing the following steps. First, at step 502, the dot spectrogram is refocused to yield a refocused dot spectrogram. Then, at step 504, a cross-correlation convolution operation is performed to yield a correlated refocused dot spectrogram. A local maxima filter \mathfrak{F} is then applied at step 506 to the

30

The calculation of Ω is independent of the oxel layout. From a preconditioning effectiveness standpoint, a best case design corresponds to a completely random oxel layout in terms of \hat{O} -value for adjacent oxels. The worst case corresponds to \hat{O} -value separation of 1 among adjacent oxels. The oxel, $o(i,j)_Z$, centered at (i,j) comprises of complementary oligonucleotides, corresponding to a mutation of interest over the set Z . Loci, r , for averaging amplitude ranges from ± 5 oxels to $\pm k$ oxels depending on $(\hat{O}\text{-value mod } 4^k)$ separation. Ω_1^Z then is computed using $\Omega_1^Z = \sum_{i-r}^{i+r} \sum_{j-r}^{j+r} \frac{\Phi(i,j)}{(2r+1)^2} \forall Z$. When the averaging loci for multiple mutations of interest overlaps, then composite loci, r' is bounded by a rectangle whose top left hand and bottom right hand corner coordinates are given by $[i_{\min}-k-1, j_{\max}+k+1]$ and $[i_{\max}+k+1, j_{\min}-k-1]$ where i_{\min} , i_{\max} , j_{\min} and j_{\max} correspond to the ordinate and abscissa for the oxel mutations with overlapping loci.

ζ given by:

$$\Phi(i,j)_l' = \Phi(i,j) - \kappa \cdot [\Omega(\Phi(i,j),k) / \sigma(\Phi(i,j),k)] \quad \forall i,j$$

The preceding expression captures local ensemble deviation from dot spectrogram average. The design parameter κ is computed offline based on specific bio-molecular signatures of interest. The suffix l denotes iterative index for a cross-correlation convolution operation to be applied after global refocusing.

A uniform dot spectrogram rescaling can be achieved by applying $\alpha \cdot \Phi(i,j)$ where α can be either a constant or a functional. This operator selectively enhances those hixels and ensemble boundaries whose intensity exceeds the local average by more than κ prespecified standard deviations.

κ is a predetermined constant computed offline based on microarray fluorescence or chemiluminescence sensitivity.

$$\kappa = \exp\left(-\sqrt{\frac{\min(\text{oligonucleotides/oxels required for fluorescent detection})}{\text{total(oligonucleotides/oxel)}}}\right)$$

The suffix l denotes an iterative index for a cross-correlation convolution operation to be applied after global refocusing.

It is given by

$$\begin{aligned} u_t + \nu Au + B(u, u) &= f, \\ u(0) &= u_0 \end{aligned}$$

- 5 where $A = -P_H \Delta$ is the Stokes operator, $B(u, u)$ stands for the non-linear term $(u \cdot \nabla)u$ projected to the underlying Hilbert space H , f is the volume force projected to the same Hilbert space and ν is the viscosity term. To meet the incompressibility condition the following Hilbert space is assumed to set the initial value problem

$$H = \left\{ u \in L^2(Q)^2 : \operatorname{div} u = 0, \int_Q u(x) dx = 0, u_i|_{x_i=L} = u_i|_{x_i=0}, j = 1, 2 \right\}$$

and

$$V = \{ u \in H^1(Q)^2 : u \in H \}$$

10

where Q is the square $[0, L] \times [0, L]$. The mathematical domain of the Stokes operator is given by

$$D(A) = H^2(Q)^2 \cap V$$

15

Galerkin Approximation can be used to approximate the exponential attractor for the system

- The above system with periodic boundary conditions admits an exponential fractal attractor
- 20 M in B whose dimensions can be estimated using

$$dF(M) \leq c G^2 (\log G^4 \nu \lambda_1 + 1)$$

where G is the Grashoff number given by $\frac{|f|}{\nu^2 \lambda_1}$ and c is a constant that depends on the shape factor. λ_1 denotes the positive eigenvalue of A .

25

The rate of convergence of this system can be computed as well.

The exponential attractor is then coupled with the post-hybridization dot spectrogram subarray

The logarithmic rescaling function is generated by generating an expansion sequence of nonnegative numbers and by generating an expanded dot spectrogram tessellation for Φ .

The expansion sequence is generated as follows:

5

$$\{\rho\} = \rho_0, \rho_1, \rho_2, \dots$$

which is strictly decreasing until it reaches zero and thereafter is equal to zero by using:

10

$$\aleph(n) = \begin{cases} 2^{n-1} & \text{for } n \geq 0 \\ 0 & \text{for } n < 0 \end{cases}$$

The expanded dot spectrogram tessellation for Φ (which is represented by $\text{DST}(\Phi)$) is generated using:

15

$$\text{DST}(\Phi) = \rho(D(\phi_i, \phi_k))$$

wherein $D(\phi_i, \phi_k)$ is a shortest possible discretized fluorescence amplitude separation between a pair of hixels ϕ_i, ϕ_k wherein ϕ_k is a local maximum.

20

The local maxima are merged into a single local maximum half way in between for downstream hixel-to-ensemble and ensemble-to-ensemble operations on hixel clusters using the sequence

25

$$\max\{\aleph(c) - \aleph(m), 0\}; \quad m = 0, 1, 2, \dots$$

where c is some positive integer constant.

Additional details are as follows, for any pair of dot spectrogram hixels, ϕ_i and ϕ_j , let the discretized fluorescence amplitude separation between them be denoted by $D(\phi_i, \phi_j)$. So, $D(\phi_i, \phi_j) = 0$ if and only if

30

$$|\phi_i - \phi_j| \leq C \text{ where } C = \text{Max}(\rho(\Phi(i,j))) - \text{Min}(\rho(\Phi(i,j)))/N \text{ and } D(\phi_i, \phi_j) = 1 \text{ if and only if } \phi_i$$

then applied to perform gradient refocusing rather than steps 502 - 510.

5 Estimation of Amplitude Wanderings

Amplitude wanderings are estimated at step 412 within the enhanced dot spectrogram. The estimate is performed by applying a Palm Distribution operator to the globally re-scaled dot spectrogram to capture amplitude wanderings and transitions at element, neighboring pair and local ensemble levels. The application of the Palm Distribution operator generates bounds that are used to accommodate degradation of hybridization over time. Essentially the estimate exploits the use of generator functions to capture stochastic variability in hybridization binding efficacy and draws upon results in stochastic integral geometry and geometric probability theory.

Geometric measures are constructed to estimate and bound the amplitude wanderings to facilitate detection. In particular we seek a measure for each mutation-recognizer centered (MRC-) hixel that is invariant to local degradation. Measure which can be expressed by multiple integrals of the form

$$m(Z) = \int_Z f(z) dz$$

where Z denotes the set of mutations of interest. In other words, we determine the function $f(z)$ under the condition that $m(z)$ should be invariant with respect to all dispersions ξ . Also, up to a constant factor, this measure is the only one which is invariant under a group of motions in a plane. In principle, we derive deterministic analytical transformations on each MRC-hixel., that map error-elliptic dispersion bound defined on \mathfrak{R}^2 (the two dimension Euclidean space - i.e., oixel layout) onto measures defined on \mathfrak{R} . The dispersion bound is given by

$$\text{Log}_4(\hat{O}_{(i,j)} |^Z).$$

Such a representation uniqueness facilitates the rapid decimation of the search space. It is implemented by instantiating a filter constructed using measure-theoretic arguments. The transformation under consideration has its theoretical basis in the Palm Distribution Theory for point processes in Euclidean spaces, as well as in a new treatment in the problem of probabilistic description of MRC-hixel dispersion generated by a geometrical processes. Latter is reduced to a

Determination of Π

Obtained by solving the inverse problem

$$\Pi = \Theta * P$$

5

where

$$P = \int_{\tau_1}^{\tau_2} \wp(\rho_{m(i,j)}, \sigma_m, \eta_m, \varpi_m) \partial \tau$$

where τ_1 and τ_2 represent the normalized hybridization dispersion limits. These number are empirically plugged in. We choose 0.1 and 0.7 respectively to signify loss of 10% - 70% hybridization.

10

Also, Θ denotes the distribution of known point process. We use the form $1/(1+\exp(\wp(\dots)))$ to represent it.

Ultimately, the final preconditioned (or enhanced) dot spectrogram generated by the step of FIG. 5 is represented by:

15

$$\tilde{\Phi}(i, j).$$

20

Resonant Interaction

Referring again to Fig. 2, at step 210, the resonant interaction between the QEF and the preconditioned dot spectrogram is performed until a pre-selected degree of convergence is

$$\overline{\alpha \dot{u}} = -\frac{\partial V(\bar{u})}{\partial \bar{u}} + \bar{\Psi}(t) + QN(t)$$

achieved. The resonance interaction proceeds by iteratively calculating a resonance equation until convergence is achieved.

25

More specifically, the following resonance equation is iteratively calculated.

$$\overline{\alpha \dot{u}} = -\frac{\partial V(\bar{u})}{\partial \bar{u}} + \bar{\Psi}(t) + QN(t)$$

electronic as well as optoelectronic QEF loading to microelectronics computing backplane, microarray readout and analysis backplane itself optoelectronically or electronically bonded to bioelectronic substrate. Furthermore the method can be implemented on offline miniature custom VLSI / palmtop / desktop setup. The QEF is also implementable in electronic, optoelectronic, bionic and ionic COTS/custom device physics. In the event the chip is designed such that complementary oligonucleotides for several mutations are spatially well spaced out that multiple QEF can be introduced to stimulate the system at the same time, then a logical "OR"ing of the resonance output is used to reach the detection decision.

Also, note that a chip fabricated to implement the exemplary method can work in two ways: a) seek all mutations of interest simultaneously; or b) seek all mutations of interest serially. An advantage of (a) over (b) is computational speedup. An advantage of (b) over (a) is serendipity, i.e., in method (a) only those mutations are resonantly amplified that are detection candidates. Everything else is likely suppressed or decimated. In (b) multiple resonant outputs can be accepted. By accepting multiple peaks for the OF the method can actually accept 2nd order, 3rd order entrained states, where order implies hamming distance to the mutation of interest in terms of base pair labels and locations. This can be used to theoretically accept entire families of derived mutations.

Preferably, the resonance interaction is performed digitally by applying a matrix representative of the resonance equation to a matrix representative of the resonance stimulus in combination with a matrix representative of the dot spectrogram.

The final result of step 210 is a set of hixel locations wherein resonance has occurred identified by row and column number (i,j).

Resonance Output Interpretation to Identify Diseases

Once resonances peak are observed in specific hixel locations of the preconditioned dot spectrogram at step 210, the hixel addresses (k,l) of those locations are mapped at step 212 into the oligonucleotide table mentioned above (which contains the oligonucleotide sequences associated with hixel locations) to thereby identify the mutations, if any, present in the sample being analyzed. This is a simple table look-up resulting in a direct readout of the mutations. For a custom POC diagnostic sensor only those hixels which relate to mutations or expressed products of interest are stored in the table.

At step 214, the mutations identified at step 212 are then mapped into the mutations table mentioned above (which contains the diseases associated with the mutations) to thereby identify the diseases, if any, present in the sample being analyzed. This is also a simple table look-up

interaction is performed. This implementation, which may also be referred to as a “mixed-mode phase shifted mode” is particularly effective for automatically extracting an entire class of mutations that may be manifested in a hybridized element. In general, the mixed-mode provides polymorphism in induced couplings for QEF design which delivers repeatability on analysis
5 whereby mutation signatures of interest are simultaneously coupled to many base “dynamical systems” with a single phase-embedding operator. Other resonance coupling interactions may be exploited as well. Other examples of couplings, other than phase-based, are “additive coupling mode” which provides further SNR enhancement and a “shunted input multiplicative coupling mode” which amplifies noise-to-noise couplings and leads to derivation of better readout threshold
10 for diagnostics decision making. Also, a combination of different resonance interactions can be exploited.

Details regarding a related implementation may be found in co-pending U.S. Patent Application 09/253,792 entitled “Method and Apparatus for Interpreting Hybridized Bioelectronic DNA Microarray Patterns Using Self Scaling Convergent Reverberant Dynamics”, is incorporated
15 by reference herein. Details regarding an implementation directed to measuring viral loads may be found in co-pending U.S. Patent Application 09/253,791 entitled “Method and Apparatus for Exponentially Convergent Therapy Effectiveness Monitoring Using DNA Microarray Based Viral Load Measurements”, is also incorporated by reference herein.

The exemplary embodiments have been primarily described with reference to flow charts
20 illustrating pertinent features of the embodiments. Each method step may also represent a hardware or software component for performing the corresponding step. It should be appreciated that not all components or method steps of a complete implementation of a practical system are necessarily illustrated or described in detail. Rather, only those components or method steps necessary for a thorough understanding of the invention have been illustrated and described in detail. Actual
25 implementations may utilize more steps or components or fewer steps or components.

The description of the exemplary embodiments is provided to enable any person skilled in the art to make or use the present invention. Various modifications to these embodiments will be readily apparent to those skilled in the art and the generic principles defined herein may be applied to other embodiments without the use of the inventive faculty. Thus, the invention is not intended
30 to be limited to the embodiments shown herein but is to be accorded the widest scope consistent with the principles and novel features disclosed herein.

re-scaling the uniformly re-scaled output pattern to amplifying local boundaries therein to yield a globally re-scaled output pattern.

6. The method of claim 5 wherein the step of re-scaling the maximized output pattern is performed by applying an operator to selectively enhance those hixels and ensemble boundaries whose intensity exceeds the local average by more than a prespecified number of standard deviations.

7. The method of claim 5 wherein the step of rescaling the uniformly re-scaled output pattern is performed by applying a logarithmic rescaling function around zero mean amplitudes within the output pattern to amplify local edge boundaries of the output pattern.

8. The method of claim 1 further including the step of estimating amplitude wanderings within the globally re-scaled output pattern.

9. The method of claim 8 wherein the step of estimating amplitude wanderings is performed by applying spectrogram ensemble invariance property generators constructed using a Palm distribution.

10. The method of claim 1 wherein the step of interpreting the resonance pattern to a yield a set of confirmed mutations by comparing resonances found therein with predetermined resonances expected for the set of mutations includes the step of mapping the confirmed mutations to known diseases associated with the pre-selected set of known mutations to identify diseases, if any, indicated by the biological sample.

11. The method of claim 1 further including the step of performing a diagnostic confirmation by taking the identified diseases and solving in reverse for the associated Quantum Expressor Functions and then comparing those Quantum Expressor Functions with ones expected for the mutations associated with the identified disease to verify correspondence and, if no correspondence is found, selecting a new sub-set of known mutations and repeating all steps.

12. The method of step 1 further including the initial steps of generating the set of nonlinear Quantum Expressor Functions by:

inputting a set of mutation signatures representative of the pre-selected set of known

19. The method of claim 1 wherein the biological sample selected from a group consisting of a DNA, RNA, protein, peptide-nucleic acid (PNA) and targeted nucleic amplification (TNA) samples.

5 20. A method for analyzing a biological sample to identify mutations, if any, present in the sample from a pre-selected set of known mutations, said method comprising the steps of:

applying the sample to a biochip to generate an output pattern representative of quantized hybridization activity of oligonucleotides in the sample;

10 selecting a sub-set of the mutations for analysis;

generating preconditioner transforms based upon the selected sub-set of mutations;

selecting a sub-set of nonlinear Quantum Expressor Functions from a set of predetermined nonlinear Quantum Expressor Functions based upon the selected sub-set of mutations;

15 preconditioning the output pattern in accordance with the preconditioner transforms to generate a modified output pattern;

iteratively processing the modified output pattern by performing a convergent reverberation to yield a resonance pattern representative of resonances between the selected set of Quantum Expressor Functions and the modified output pattern until a pre-selected degree of convergence is achieved between resonances of the resonance pattern and mutations of the selected sub-set of mutations; and

20

interpreting the resonance pattern to yield a set of confirmed mutations by comparing the resonances therein with resonances expected for the mutations of the selected set of mutations.

21. The method of claim 20 further including the step of mapping the confirmed mutations to known diseases associated with the pre-selected set of known mutations to identify diseases, if any, indicated by the biological sample.

25

22. A method of generating a set of nonlinear Quantum Expressor Functions comprising the steps of:

30 inputting a set of mutation signatures representative of the pre-selected set of known mutations;

inputting a representation of a biochip;

generating a set of resonant interaction parameters representative of mutation pattern interactions between elements of the biochip including interactions from a group including

yield a globally re-scaled output pattern.

27. The system of claim 23 wherein the resonance pattern interpretation unit is operative to map the confirmed mutations to known diseases associated with the pre-selected set of known mutations to identify diseases, if any, indicated by the biological sample.

28. The system of step 23 further including a Quantum Expressor Function generator operative to:

- input a set of mutation signatures representative of the set of known mutations;
- 10 input a representation of a biochip microarray pattern layout for the biochip from which the output pattern is generated;
- generate a set of resonant interaction parameters representative of mutation pattern interactions between elements of the biochip including interactions from a group including element-to-element interactions, element-to-ensemble interactions, ensemble-to-element
- 15 interactions, and ensemble-to-ensemble interactions; and
- generate the set of nonlinear Quantum Expressor Functions from the set of resonant interaction patterns.

29. The system of claim 23 wherein the output pattern is a quantized output pattern.

20 30. The system of claim 29 wherein the quantized output pattern is a dot spectrogram.

31. The system of claim 29 wherein the biological sample is selected from a group consisting of a DNA, RNA, protein, peptide-nucleic acid (PNA) and targeted nucleic amplification (TNA) samples.

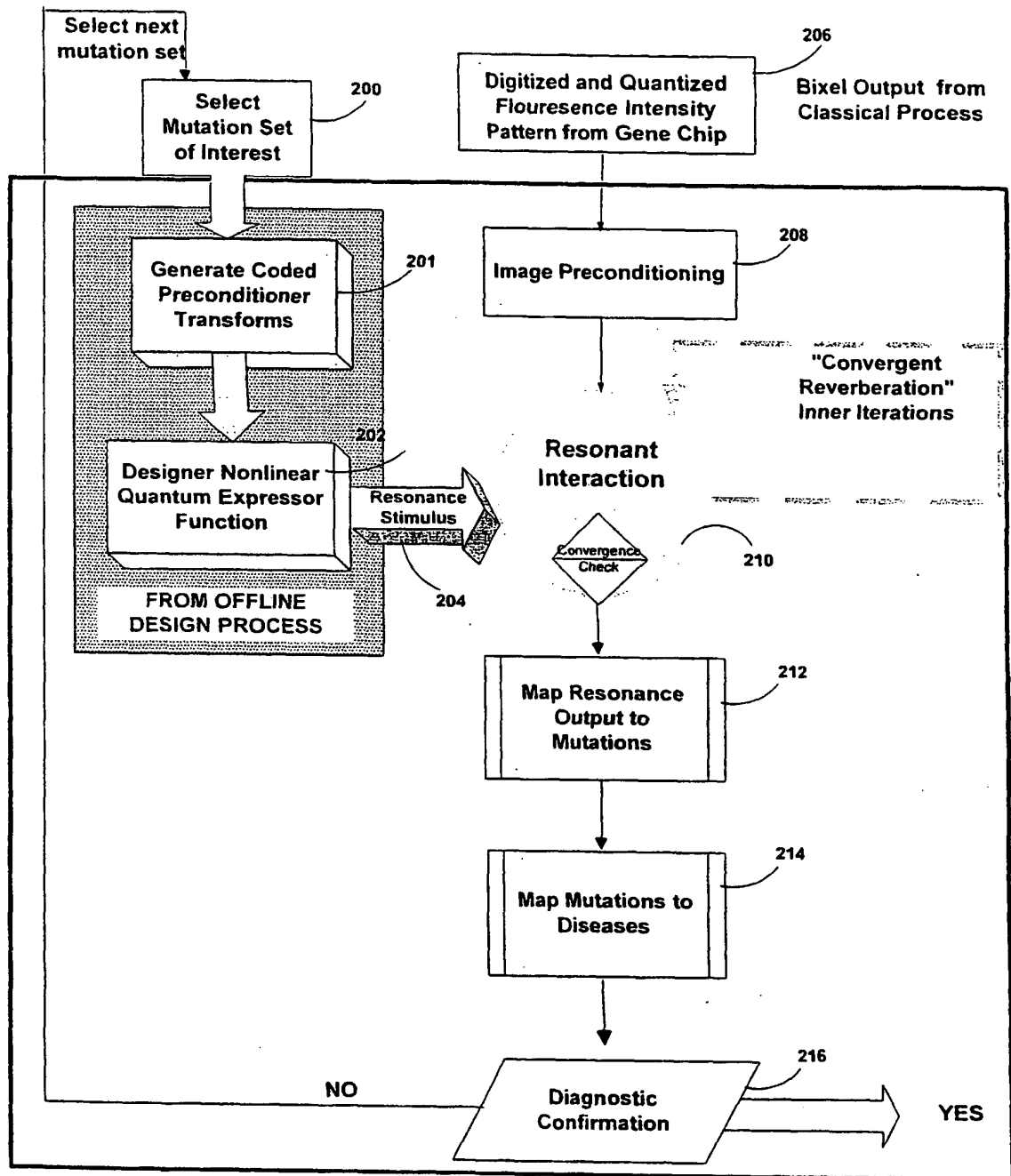
32. A system of generating a set of nonlinear Quantum Expressor Functions based upon a set of mutation signatures representative of a set of known mutations and based upon a biochip microarray pattern, said system comprising:

- a resonant interaction parameter generator operative to generate a set of resonant interaction parameters representative of mutation pattern interactions between elements of the biochip including interactions from a group including element-to-element interactions, element-to-ensemble interactions, ensemble-to-element interactions, and ensemble-to-ensemble interactions;
- 30 and

a Quantum Expressor Functions generator operative to generate a set of nonlinear Quantum Expressor Functions from the set of resonant interaction patterns.

2/5

FIGURE 2



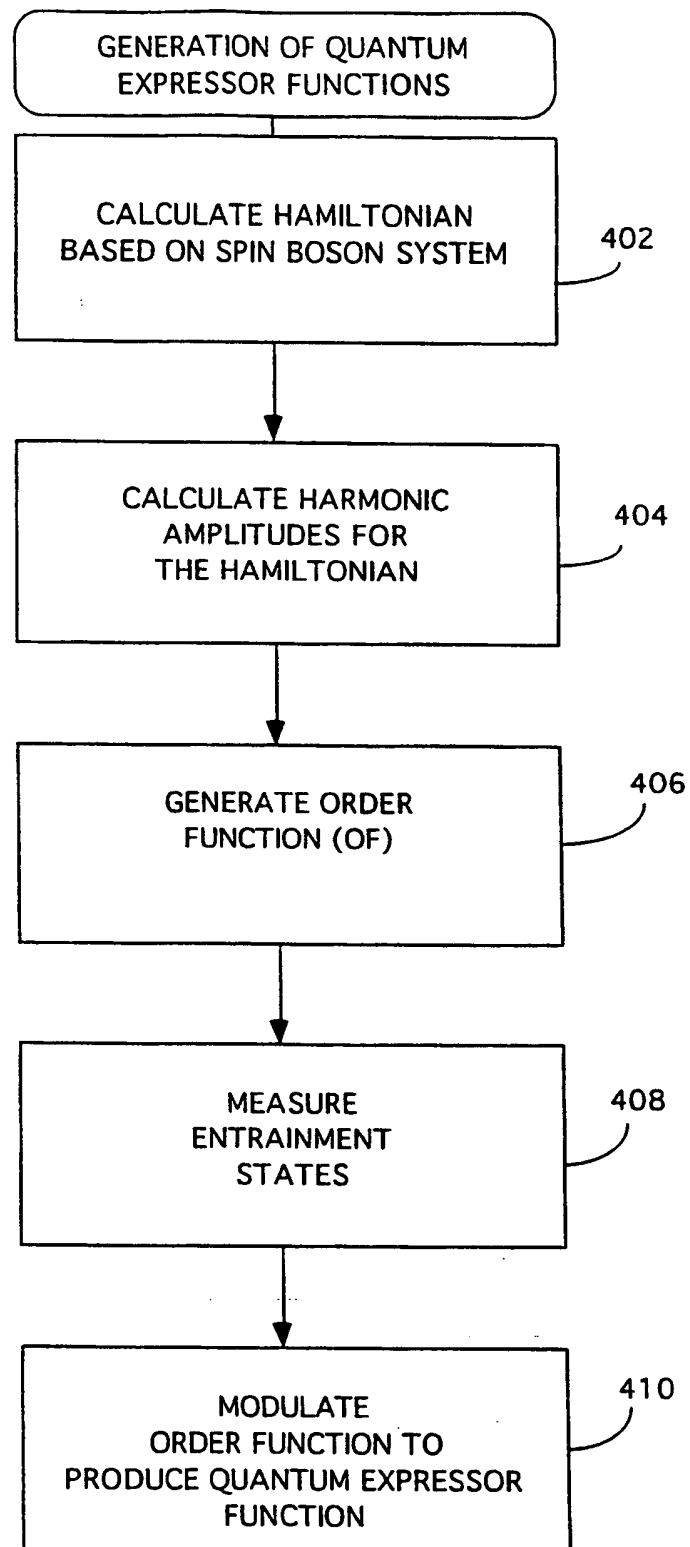


FIG. 4

(19) World Intellectual Property Organization
International Bureau



(43) International Publication Date
8 September 2000 (08.09.2000)

PCT

(10) International Publication Number
WO 00/52625 A3

(51) International Patent Classification⁷: G06F 19/00

(74) Agents: KUKKONEN, Carl, A., III et al.; Pretty, Schroeder & Poplawski, 19th floor, 444 South Flower Street, Los Angeles, CA 90071 (US).

(21) International Application Number: PCT/US00/04076

(22) International Filing Date: 17 February 2000 (17.02.2000)

(25) Filing Language: English

(26) Publication Language: English

(30) Priority Data:
09/253,789 22 February 1999 (22.02.1999) US

(71) Applicant (for all designated States except US): VIAL-OGY CORPORATION [US/US]; 2400 Lincoln Avenue, Altadena, CA 91001 (US).

(72) Inventor; and

(75) Inventor/Applicant (for US only): GULATI, Sandeep [IN/US]; 5467 La Forest Drive, La Canada, CA 91011 (US).

(81) Designated States (national): AE, AL, AM, AT, AU, AZ, BA, BB, BG, BR, BY, CA, CH, CN, CR, CU, CZ, DE, DK, DM, EE, ES, FI, GB, GD, GE, GH, GM, HR, HU, ID, IL, IN, IS, JP, KE, KG, KP, KR, KZ, LC, LK, LR, LS, LT, LU, LV, MA, MD, MG, MK, MN, MW, MX, NO, NZ, PL, PT, RO, RU, SD, SE, SG, SI, SK, SL, TJ, TM, TR, TT, TZ, UA, UG, US, UZ, VN, YU, ZA, ZW.

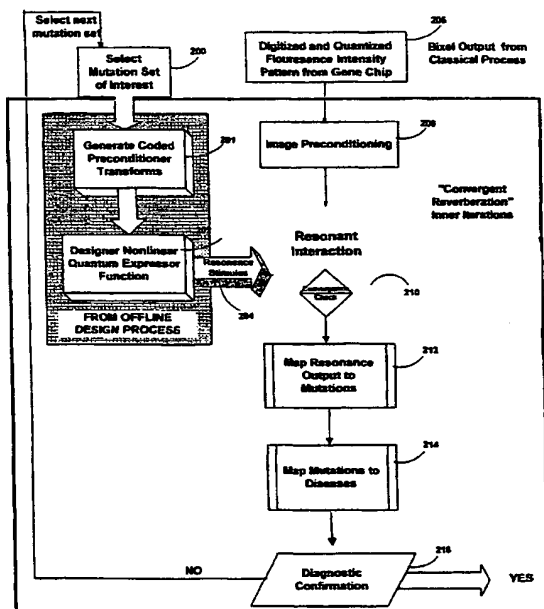
(84) Designated States (regional): ARIPO patent (GH, GM, KE, LS, MW, SD, SL, SZ, TZ, UG, ZW), Eurasian patent (AM, AZ, BY, KG, KZ, MD, RU, TJ, TM), European patent (AT, BE, CH, CY, DE, DK, ES, FI, FR, GB, GR, IE, IT, LU, MC, NL, PT, SE), OAPI patent (BF, BJ, CF, CG, CI, CM, GA, GN, GW, ML, MR, NE, SN, TD, TG).

Published:

— With international search report.

[Continued on next page]

(54) Title: METHOD AND APPARATUS FOR ANALYZING HYBRIDIZED BIOCHIP PATTERNS USING RESONANCE INTERACTIONS



(57) Abstract: A technique is described for identifying mutations, if any, present in a biological sample, from a pre-selected set of known mutations. The method can be applied to DNA, RNA and peptide nucleic acid (PNA) microarrays. The method analyzes a dot spectrogram representative of quantized hybridization activity of oligonucleotides in the sample to identify the mutations. In accordance with the method, a resonance pattern is generated which is representative of nonlinear resonances between a stimulus pattern associated with the set of known mutations and the dot spectrogram. The resonance pattern is interpreted to yield a set of confirmed mutations by comparing resonances found therein with predetermined resonances expected for the selected set of mutations. In a particular example, the resonance pattern is generated by iteratively processing the dot spectrogram by performing a convergent reverberation to yield a resonance pattern representative of resonances between a predetermined set of selected Quantum Expressor Functions and the dot spectrogram until a predetermined degree of convergence is achieved between the resonances found in the resonance pattern and resonances expected for the set of mutations. The resonance pattern is analyzed to yield a set of confirmed mutations by mapping the confirmed mutations to known diseases associated with the pre-selected set of known mutations to identify diseases, if any, indicated by the biological sample. By exploiting a resonant interaction,

mutation signatures may be robustly identified even in circumstances involving low signal to noise ratios or, in some cases, negative signal to noise ratios.

INTERNATIONAL SEARCH REPORT

International Application No

PCT/US 00/04076

A. CLASSIFICATION OF SUBJECT MATTER

IPC 7 G06F19/00

According to International Patent Classification (IPC) or to both national classification and IPC

B. FIELDS SEARCHED

Minimum documentation searched (classification system followed by classification symbols)

IPC 7 G06F

Documentation searched other than minimum documentation to the extent that such documents are included in the fields searched

Electronic data base consulted during the international search (name of data base and, where practical, search terms used)

EPO-Internal, INSPEC, WPI Data

C. DOCUMENTS CONSIDERED TO BE RELEVANT

Category *	Citation of document, with indication, where appropriate, of the relevant passages	Relevant to claim No.
A	BROWN P O ET AL: "EXPLORING THE NEW WORLD OF THE GENOME WITH DNA MICROARRAYS" NATURE GENETICS,US,NEW YORK, NY, vol. 21, no. SUPPL, January 1999 (1999-01), pages 33-37, XP000865984 ISSN: 1061-4036 abstract page 35, left-hand column, paragraph 2 ---	1-32
A	WO 98 48048 A (BALASUBRAMANIAN SHANKAR ;UNIV CAMBRIDGE TECH (GB)) 29 October 1998 (1998-10-29) abstract; claim 1 --- -/--	1-32

☒ Further documents are listed in the continuation of box C.☒ Patent family members are listed in annex.

* Special categories of cited documents :

"A" document defining the general state of the art which is not considered to be of particular relevance

"E" earlier document but published on or after the international filing date

"L" document which may throw doubts on priority claim(s) or which is cited to establish the publication date of another citation or other special reason (as specified)

"O" document referring to an oral disclosure, use, exhibition or other means

"P" document published prior to the international filing date but later than the priority date claimed

"T" later document published after the international filing date or priority date and not in conflict with the application but cited to understand the principle or theory underlying the invention

"X" document of particular relevance; the claimed invention cannot be considered novel or cannot be considered to involve an inventive step when the document is taken alone

"Y" document of particular relevance; the claimed invention cannot be considered to involve an inventive step when the document is combined with one or more other such documents, such combination being obvious to a person skilled in the art.

"&" document member of the same patent family

Date of the actual completion of the international search

3 October 2000

Date of mailing of the international search report

09/10/2000

Name and mailing address of the ISA

European Patent Office, P.B. 5818 Patentaan 2
NL - 2280 HV Rijswijk
Tel. (+31-70) 340-2040, Tx. 31 651 epo nl,
Fax: (+31-70) 340-3016

Authorized officer

Filloy Garcia, E

INTERNATIONAL SEARCH REPORT

Information on patent family members

International Application No

PCT/US 00/04076

Patent document cited in search report	Publication date	Patent family member(s)	Publication date
WO 9848048 A	29-10-1998	AU 7064198 A	13-11-1998
WO 9837417 A	27-08-1998	AU 6169098 A	09-09-1998
		EP 0979409 A	16-02-2000
US 5784162 A	21-07-1998	US 5539517 A	23-07-1996
		EP 0830564 A	25-03-1998
		JP 11500832 T	19-01-1999
		US 6075599 A	13-06-2000
		WO 9721979 A	19-06-1997
		US 6066459 A	23-05-2000
		US 6007996 A	28-12-1999
		US 5936731 A	10-08-1999
		US 5817462 A	06-10-1998
		US 5719024 A	17-02-1998
		US 5856871 A	05-01-1999
		US 5991028 A	23-11-1999
		US 5835214 A	10-11-1998
		US 5798262 A	25-08-1998
		US 6018587 A	25-01-2000
		US 6055325 A	25-04-2000
		US 5912165 A	15-06-1999
		US 5906919 A	25-05-1999
		EP 0767361 A	09-04-1997
US 3786341 A	15-01-1974	CA 993511 A	20-07-1976
		CH 558014 A	15-01-1975
		DE 2351671 A	02-05-1974
		GB 1446563 A	18-08-1976
		JP 1182539 C	27-12-1983
		JP 49096790 A	12-09-1974
		JP 58012543 B	09-03-1983